Journal of Molecular Catalysis A: Chemical 416 (2016) 29–38

Contents lists available at ScienceDirect

Journal of Molecular Catalysis A: Chemical

journal homepage: www.elsevier.com/locate/molcata

Application of arene ruthenium(II) complexes with pyridine-2-carboxaldimine ligands in the transfer hydrogenation of ketones

Joel M. Gichumbi, Holger B. Friedrich*, Bernard Omondi

School of Chemistry, University of Kwazulu-Natal, Private Bag X54001, Durban 4001, South Africa

ARTICLE INFO

Article history:
Received 11 December 2015
Received in revised form 9 February 2016
Accepted 10 February 2016
Available online 12 February 2016

Keywords:
Ru(II) arene complexes
Transfer hydrogenation
Pyridine-imine ligands

ABSTRACT

The reaction of various pyridine-2-carboxaldimine ligands with the $[(\eta^6\text{-arene})Ru(\mu\text{-Cl})Cl]_2$ dimer followed by a metathesis reaction with ammonium hexaflourophosphate, yielded the ruthenium(II) arene complex salts $[(\eta^6\text{-arene})RuCl(C_5H_4N\text{-}2\text{—}CH{=}N\text{-}Ar]PF_6$; where (arene = C_6H_6 (**1**), *p*-cymene (**2**), Ar = 3, 5-dimethyl phenyl (**a**), 2,3-dimethyl phenyl (**b**), 2,5-dimethyl phenyl (**c**), 3,4-dimethyl phenyl (**d**)). The compounds were characterized by elemental analysis, FT- IR, UV–vis and ^1H and ^{13}C NMR. Single crystal X-ray structures for compounds **1a**, **1d** and **2e** were also determined and showed that the ruthenium(II) centre has a pseudo-octahedral geometry and the molecule adopted a three legged piano stool geometry in which the arene ring occupies the apex and the nitrogen atoms of the *N*,*N′*-bidentate ligand and the chloride atom the base of the stool. The Ru(II) complex salts were active for the catalytic transfer hydrogenation of ketones into alcohols in the presence of NaOH using 2-propanol as the hydrogen source at 82 °C. The complexes were suitable for a wide range of aliphatic, cyclic and aromatic ketones giving good turn over numbers.

© 2016 Elsevier B.V. All rights reserved.

1. Introduction

Catalytic transfer hydrogenation is the selective reduction of multiple bonds with the aid of an organic molecule as the hydrogen donor in the presence of a catalyst [1] and is a useful fundamental reaction in chemistry used in a number of chemical processes [2–4]. For example, the catalytic hydrogenations of carbon–carbon double bonds of alkenes, carbon-hetero atom double bonds of ketones, aldehydes and imines has become an indispensable processes for the production of a wide range of alkanes, alcohols and amines, including chiral compounds. These value added products are used as precursors for the pharmaceutical, agrochemical, flavor, fragrance, material and fine chemical industries [5,6].

In addition, transfer hydrogenation of carbonyl compounds is a preferred industrial and laboratory reaction because of the ease of carrying out the reaction and the relatively low cost [7,8] as no free hydrogen is used, hence, no special hydrogen storage, monitoring and dispensing equipment are required [9]. Hydrogen donors used in transfer hydrogenation are usually secondary alcohols, in particular isopropanol and triethyl ammonium formate ($HCOOH/NHEt_3$) [10].

The most active and selective hydrogen transfer catalysts are ruthenium, rhodium and iridium complexes [11]. Ruthenium complexes are preferable over those of rhodium and iridium because of their high activity and lower cost. Among the different ruthenium compounds, arene ruthenium compounds belong to a well-established family of robust metal-organic molecules that have played an important role in the development of organometallic chemistry. They have attracted a lot of interest due to their catalytic potential in a wide range of organic reactions [12–15] and also display promising anticancer activity [16–20]. The arene ruthenium $[(\eta^6\text{-arene})Ru(\mu\text{-Cl})Cl]_2$ dimers have been found to undergo cleavage of the chloride bridges with various monodentate ligands (L) to give the monomeric compounds $[(\eta^6\text{-arene})RuCl_2L]$ (L = monodentate donor) [21]. Further halide substitution may afford the cationic derivatives $[(\eta^6\text{-arene})RuClL_2]^+$ with bidentate (L_2) donors [21].

The presence of the aromatic π-ligand as part of the ruthenium complex stabilizes and protects the metal center, preventing rapid oxidation to Ru(III). Moreover, the arene ligands are relatively inert towards substitution reactions and consequently are often considered as spectator ligands. However, the arene moiety which is strongly coordinated to the ruthenium, can be customized

* Corresponding author. Fax: +27 312603091.
E-mail addresses: friedric@ukzn.ac.za, holgerbfriedrich@gmail.com (H.B. Friedrich).

http://dx.doi.org/10.1016/j.molcata.2016.02.012
1381-1169/© 2016 Elsevier B.V. All rights reserved.

by simply attaching different substituents. These functionalized substituents can be modified to tune the properties of the arene ruthenium complexes. The three remaining coordination sites opposite the arene ligand can be used to introduce a wide variety of ligands with N-, O-, S- or P donor atoms. The resulting complexes are neutral, mono or dicationic and often form metal-donor atom bonds useful for catalytic reactions [22–24].

Nitrogen based ligands are popular in coordination chemistry because they are easily modified both sterically and electronically [25,26]. Significant information can be obtained by investigating the effect of ligand structure on the properties of transition metal complexes [18–20]. Pyridine-imines belong to the diimine class of nitrogen based ligands and they are known to bind metal ions as *N*,*N*′-donors forming stable five membered chelate rings. In these *N*,*N*′-donor ligands both the nitrogen donating fragments, i.e. the pyridyl fragments and the imine fragments, have considerable π-acid character and hence complexation to the ruthenium centre stabilizes the bivalent state of the ruthenium to a significant extent and thereby enhance the reactivity of the arene moiety [27]. In this study the application of new half-sandwich arene (arene = benzene or *p*-cymene) ruthenium complexes with nitrogen based pyridine-imine ligands for the transfer hydrogenation of ketones are reported.

2. Experimental

2.1. General procedures

All experimental manipulations of organometallic compounds were carried out under inert atmosphere using standard Schlenk line techniques unless otherwise stated. Reagent grade hexane and Et_2O were distilled from sodium/benzophenone and used immediately; acetone and MeCN were distilled from anhydrous $CaCl_2$ and stored under molecular sieves of porosity size 4 Å. The other reagents were used as received from the suppliers without further purification. Melting points were recorded on an Ernest Leitz Wetzlar hot-stage microscope. High and low resolution mass spectra were recorded on a Waters micromass LCT premier TOF-MS. Elemental analyses were recorded on a ThermoScientific Flash 2000 elemental analyzer. Infrared spectra were recorded using an ATR PerkinElmer Spectrum 100 spectrometer between 4000–400 cm^{-1}. Thermogravimetric analysis (TGA) was performed on a SDTQ600 TGA–DSC in a nitrogen atmosphere. Electronic spectra were recorded in acetonitrile with a PerkinElmer Lamba 35 UV–vis spectrophotometer with 10 mm path length quartz cuvettes. ^1H and ^{13}C NMR spectra were recorded using Bruker 400 MHz spectrometers and chemical shifts are recorded in ppm. The deuterated solvent DMSO-d_6 was used as purchased. The transfer hydrogenation reaction was monitored by gas chromatography (GC) with an Agilent Capillary GC model 6820 fitted with a DB wax polyethylene column (0.25 mm in diameter, 30 m in length), a flame ionization detector and nitrogen gas at a flow rate of 2 ml/min. Reagents were purchased from Aldrich or Merck and were used as received. The precursors $[(\eta^6\text{-}C_6H_6)Ru(\mu\text{-}Cl)Cl]_2$ and $[(\eta^6\text{-}p\text{-cymene})Ru(\mu\text{-}Cl)Cl]_2$ were prepared according to reported procedures [28]. The pyridine-imine ligands (3,5-dimethyl-phenyl)-pyridin-2-yl methylene amine (**a**), (2,3-dimethyl-phenyl)-pyridin-2-yl methylene amine (**b**), (2,5-dimethyl-phenyl)-pyridin-2-yl methylene amine (**c**), (3,4-dimethyl-phenyl)-pyridin-2-yl methylene amine (**d**), were prepared according to methods reported in literature [29].

2.2 Synthesis and characterization of cationic mononuclear Ru(II) iminopyridyl complexes $[(\eta^6\text{-}C_6H_6)ruCl\ (C_5H_4N\text{-}2\text{—}CH{=}N\text{-}Ar]\ PF_6$

Compounds **1a–d** were prepared using a general procedure described below. A mixture of $[(\eta^6\text{-}C_6H_6)Ru(\mu\text{-}Cl)Cl]_2$ (100 mg, 0.20 mmol), ligand a in slight excess (88.3 mg, 0.42 mmol) and 2.5 equivalents of NH_4PF_6 (82 mg, 0.5 mmol) in dry methanol 20 ml were stirred at ambient temperature for three hours. The precipitate formed was separated by filtration, washed with diethyl ether and dried *in vacuo*.

1a

Orange powder. Yield 70%. m.p.: 200.3 °C (decomp.) ^1H NMR (400 MHz, DMSO-d_6): δ 9.65 (*d*, J_{HH} = 5.28 Hz, 1H, Py); 8.87 (*s*, 1H, CH=N); 8.29 (*m*, 2H, Py); 7.88 (*t*, 1H, Py); 7.39 (*s*, 2H, Ar); 7.21 (*s*, 1H, Py), 5.95 (*s*, 6H, C_6H_6); 2.4 (*s*, 6H, CH_3). ^{13}C NMR (600 MHz, DMSO-d_6): δ 168.1 (CH=N); δ 156.7 (py); δ 152.5 (py); δ 140.5 (py); δ 139.3 (py); δ 131.5 (py); δ 130.5 (py); δ 130.31 (py); δ 129.16 (Ar); δ 120.4 (Ar); δ 87.870 (C_6H_6); 21.4 (CH_3). IR (KBr, cm^{-1}): 1609 (—CH=N), 828 (P-F). Anal. Calcd for $[C_{20}H_{20}ClN_2Ru]PF_6$ C, 42.15; H, 3.54; N, 4.92. Found: C, 42.11; H, 3.705; N, 5.03. MS (ESI, *M*/*Z*): 425.0363 for $[C_{20}H_{20}ClN_2Ru]^+$

1b

The procedure described above for **1a** was used except ligand **b** was used (88 mg, 0.42 mmol).

Orange powder. Yield 73%. m.p.: 195.5 °C (decomp.) ^1H NMR (400 MHz, DMSO-d_6): δ 9.68 (*d*, J_{HH} = 5.32 Hz, 1H, Py); 8.81(*s*, 1H, CH=N); 8.32 (*m*, 2H, Py); 8.24 (*m*, 1H, Py); 7.91(*s*, 1H, Ar); 7.35 (*m*, 2H, Ar), 5.88 (*s*, 6H, C_6H_6); 2.40 (*s*, 3H, CH_3), 2.26 (*s*, 3H, CH_3). ^{13}C NMR (400 MHz, DMSO- d_6): δ 171.52 (CH=N); δ 156.8 (py); δ 154.8 (py); δ 140.6 (py); δ 139.1(py); δ 130.3 (py); δ 129.34 (py); δ 126.50 (py); δ 87.79 (C_6H_6); 20.78 (CH_3). IR (KBr, cm^{-1}): 1618 (—CH=N), 830.03 (P-F). Anal. Calcd for $[C_{20}H_{20}ClN_2Ru]PF_6$ C, 42.15; H, 3.54; N, 4.92. Found: C, 42.39; H, 3.54; N, 5.032 MS (ESI, *M*/*Z*): 425.0341 for $[C_{20}H_{20}ClN_2Ru]^+$

1c

The procedure described above for **1a** was used except ligand **c** was used (88 mg, 0.42 mmol).

Orange powder. Yield 75%. m.p.: 207.8 °C (decomp.) ^1H NMR (400 MHz, DMSO-d_6): δ 9.67 (*d*, J_{HH} = 5.36 Hz, 1H, Py); 8.84 (s, 1H, CH=N); 8.32 (*d*, J_{HH} = 7.48 Hz, 1H, Py); 8.24 (*d*, J_{HH} = 7.36 Hz, 1H, Py); 7.91(t, 1H,Py); 7.48 (*s*, 1H, Ar), 7.38 (*d*, J_{HH} = 7.88 Hz 1H, Ar), 7.24 (*d*, J_{HH} = 7.68, 1H, Ar), 5.89 (*s*, 6H, C_6H_6); 2.36 (*s*, 3H, CH_3), 2.33 (*s*, 3H, CH_3). ^{13}C NMR (400 MHz, DMSO- d_6): δ 170.88 (CH=N); δ 156.24 (py); δ 151.47 (py); δ 140.07 (py); δ 136.20 (py); δ 131.36 (py); δ 130.03 (Ar); δ 129.36 (Ar); δ 128.88 (Ar); δ 122.93 (Ar); δ 87.87 (C_6H_6); δ 20.59 (CH_3); δ 20.59 (CH_3). IR (KBr, cm^{-1}): 1617 (—CH=N), 826.50 (P-F). Anal. Calcd for $[C_{20}H_{20}ClN_2Ru]PF_6$ C, 42.15; H, 3.54; N, 4.92. Found: C, 41.73; H, 3.55; N, 4.962.MS (ESI, *M*/*Z*): 425.0356 for $[C_{20}H_{20}ClN_2Ru]^+$

1d

The procedure described above for **1a** was used except ligand **d** was used (88 mg, 0.42 mmol).

Orange powder. Yield 70%. m.p.: 205.5 °C (decomp.) ^1H NMR (400 MHz, DMSO-d_6): δ 9.65 (*d*, J_{HH} = 5.4 Hz, 1H, Py); 8.86(*s*, 1H, CH=N); 8.29 (*m*, 2H, Py); 7.88 (*m*, 1H, Py); 7.57(d, J_{HH} = 6.48 Hz, 2H, Ar); 7.38(d, J_{HH} = 8.6 Hz, 1H, Ar), 5.95 (*s*, 6H, C_6H_6); 2.36 (*d*, J_{HH} = 7.24 Hz, 6H, $2CH_3$). ^{13}C NMR (400 MHz, DMSO- d_6): δ 166.94 (CH=N); δ 156.5 (py); δ 154.69 (py); δ 149.76 (py); δ 139.99 (py); δ 138.31(py); δ 13753 (Ar); δ 129.68 (Ar); δ 128.56 (Ar); δ 122.73 (Ar); δ 120.2 (Ar); δ 87.25 (C_6H_6); δ 19.53 (CH_3); δ 19.16 (CH_3). IR (KBr, cm^{-1}): 1602 (—CH=N), 832.47 (P-F). Anal. Calcd for $[C_{20}H_{20}ClN_2Ru]PF_6$ C, 42.15; H, 3.54; N, 4.92. Found: C, 41.92; H, 3.47; N, 4.78. MS (ESI, *M*/*Z*): 425.0364 for $[C_{20}H_{20}ClN_2Ru]^+$

2.3 Synthesis and characterization of cationic mononuclear complex $[(\eta^6\text{-}p\text{-cymene})RuCl\ (C_5H_4N\text{-}2\text{—}CH{=}N\text{-}\ Ar]PF_6$

Compounds **2a–d** were prepared using a general procedure described below. A mixture of the precursor complex $[(\eta^6\text{-}p\text{-cymene})Ru(\mu\text{-}Cl)Cl]_2$ (100 mg, 0.163 mmol) and the ligand a in slight excess (74 mg, 0.35 mmol) dissolved in DCM was stirred for three hours at ambient temperature. The solvent was then evaporated to dryness, giving a yellow oil that was treated with NH_4PF_6

(80 mg, 0.42 mmol) in 10 ml ethanol. The mixture was stirred in an ice bath maintained at zero degrees for two hours resulting in orange or yellow solids, isolated by gravity filtration, washed with diethyl ether and dried *in vacuo*.

2a

Orange powder, yield 83%, m.p. 190.0 °C (decomp.) ^{1}H NMR (400 MHz, DMSO-d_6): δ 9.56 (*d*, J_{HH} = 5.4 Hz, 1H, Py); 8.88 (*s*, 1H, CH=N); 8.30 (*m*, 2H, Py); 7.89 (*m*, 1H, Py); 7.38 (*s*, 2H, Ar); 7.22(*s*, 1H, Ar), 6.02 (d, J_{HH} = 6.24 Hz,1H, *p*-cymene); 5.74(d, J_{HH} = 6.20 Hz, 1H, *p*-cymene); 5.65 (*d*, J_{HH} = 6.12 Hz, 1H, Ar, *p*-cymene); 5.56 (*d*, J_{HH} = 6.12 Hz, 1H, Ar, *p*-cymene), 2.50 (*m*, 1H, C*H*(CH_3)$_2$); 2.40 (*s*, 3H, *p*-Me (cymene)); 2.13 (*m*, 6H, C*H*-Me$_2$ (cymene)); 1.01(m,6H,2CH_3). ^{13}C NMR (400 MHz, DMSO-d_6). δ 167.3 (C_2-Py), 155.9 (CH=N), 155.5(Py); 151.9 (Py); 139.9 (Py); 138.8 (Py); 129.44 (Ar); 131.1(Ar); 129.8 (Ar); 128.8 (Ar);119.9 (Ar);105.5 (Ar); 86.3 (Ar, *p*-cymene); 85.8 (Ar, *p*-cymene)); 85.6 (Ar, *p*-cymene)) 85.3 (Ar, *p*-cymene)) 30.4 (CH_3- *p*-cymene); 21.7 (CH_3, *p*-cymene); 21.3 (CH_3, *p*-cymene); 20.89 (CH_3, *p*-cymene); 18.1(CH_3). IR (KBr, cm^{-1}): 1608 (—CH=N), 828 (P-F). Anal. Calcd for [$C_{24}H_{28}ClN_2Ru$] PF_6 C, 46.05; H, 4.51; N, 4.48. Found: C, 45.98; H, 3.80; N, 4.51 MS (ESI, *M*/*Z*): 481.0981 for [$C_{24}H_{28}ClN_2Ru$] $^+$

2b

The procedure described above for **2a** was used except ligand **b** was used (74 mg, 0.35 mmol).

Orange powder, yield 82%, m.p. 193.5 °C (decomp.) ^{1}H NMR (400 MHz, DMSO-d_6): δ 9.62 (*d*, J_{HH} = 5.36 H Hz, 1H, Py); 8.83 (*s*, 1H, CH=N); 8.24 (*m*, 1H, Py); 7.93 (*m*, 1H, Py); 7.52 (*s*, 1H, Ar); 7.34 (*s*, 2H, Ar), 5.98 (*s*, 1H, *p*-cymene); 5.72 (*d*, J_{HH} = 6.16 H Hz, 2H, *p*-cymene); 5.28 (*s*, 1H, Ar, *p*-cymene); 2.61 (*m*, 1H, C*H*(CH_3)$_2$); 2.41 (*s*, 3H, *p*-Me(cymene)); 2.26 (*s*, 3H, CH-Me (cymene)); 2.08 (*s*, 3H, CH-Me (cymene)); 1.02 (*m*, 6H, 2CH_3). ^{13}C NMR (400 MHz, DMSO-d_6). δ 171.1930 (C_2-Py), 156.5 (CH=N), 154.8(Py); 140.48 (Py); 139.12 (Py); 130.57 (Py); 130.30 (Ar); 129.63 (Ar); 126.4 (Ar); 120.8 (Ar); 101.8(Ar); 86.3 (Ar, *p*-cymene); 87.4 (Ar, *p*-cymene)); 30.8 (CH_3- *p*-cymene); 22.6 (CH_3, *p*-cymene); 21.6 (CH_3, *p*-cymene); 20.8 (CH_3, *p*-cymene); 18.5(CH_3). IR (KBr, cm^{-1}): 1618 (—CH=N), 829 (P-F). Anal. Calcd for [$C_{24}H_{28}ClN_2Ru$] PF_6 C, 46.05; H, 4.51; N, 4.48. Found: C, 45.40; H, 4.68; N, 4.23. MS (ESI, *M*/*Z*): 481.0997 for [$C_{24}H_{28}ClN_2Ru$]$^+$

2c

The procedure described above for **2a** was used except ligand **c** was used (74 mg, 0.35 mmol).

Orange powder, yield 85%, m.p. 207.0 °C (decomp.) ^{1}H NMR (400 MHz, DMSO-d_6): δ 9.62 (*d*, J_{HH} = 5.28 Hz, 1H, Py); 8.87 (*s*, 1H, CH=N); 8.34(*m*, 2H, Py); 7.93 (*t*, 1H, Py); 7.39 (*d*, J_{HH} = 7.76 Hz, 1H, Ar); 7.26 (*d*, J_{HH} = 7.64 Hz, 1H, Ar), 5.95(*d*, J_{HH} = 5.96 Hz, 2H, *p*-cymene); 5.73(*d*, J_{HH} = 6.00 Hz, 2H, *p*-cymene); 5.34(*d*, J_{HH} = 4.92 Hz, 1H, Ar, *p*-cymene); 2.51 (*m*, 1H, C*H*(CH_3)$_2$); 2.36 (*d*, J_{HH} = 10.84 Hz, 6H, CH-Me$_2$ (cymene)); 2.09 (*s*, 3H, *p*-Me (cymene)); 1.05(*d*, J_{HH} = 6.72HZ, 3H,CH_3); 0.96 (*d*, J_{HH} = 6.80 Hz, 3H,CH_3). ^{13}C NMR (400 MHz, DMSO-d_6). δ 170.43 (C_2-Py), 154.35 (CH=N), 151.18(Py); 140.01(Py); 136.05(Py); 131.43(Py); 130.01(Ar); 129.17(Ar); 123.24(Ar); 105.73(Ar);100.66 (Ar); 87.27 (Ar, *p*-cymene); 86.91 (Ar, *p*-cymene)); 86.36 (Ar, *p*-cymene); 30.38 (CH_3- *p*-cymene); 22.02 (CH_3, *p*-cymene); 20.93 (CH_3, *p*-cymene); 20.49 (CH_3, *p*-cymene); 17.89 (CH_3); 17.13 (CH_3). IR (KBr, cm^{-1}): 1611 (—CH=N), 829 (P-F). Anal. Calcd for [$C_{24}H_{28}ClN_2Ru$] PF_6 C, 46.05; H, 4.51; N, 4.48. Found: 45.62; H, 4.02; N, 4.58. MS (ESI, *M*/*Z*): 481.0993 for [$C_{24}H_{28}ClN_2Ru$]$^+$

2d

The procedure described above for **2a** was used except ligand **d** was used (74 mg, 0.35 mmol).

Yellow powder, yield 82%, m.p. 198.0 °C (decomp.) ^{1}H NMR (400 MHz, DMSO-d_6): δ 9.56 (*d*, J_{HH} = 5.44 Hz,1H, Py); 8.87 (*s*, 1H, CH=N); 8.29 (*m*, 2H, Py); 7.87(*m*, 1H, Py); 7.55 (*m*, 2H, Ar); 7.38(*m*, 1H, Ar), 6.06(*d*, J_{HH} = 6.24 Hz,1H, *p*-cymene); 5.74(*d*, J_{HH} = 6.2 Hz,1H, *p*-cymene); 5.63 (*d*, J_{HH} = 6.12 Hz, 1H, Ar, *p*-cymene); 5.56 (*d*, J_{HH} = 6.12 Hz, 1H, Ar, *p*-cymene); 2.61 (*m*, 1H, C*H*(CH_3)$_2$), 2.35 (*d*, J_{HH} = 6.56 Hz, 6H, CH-Me$_2$ (cymene)); 2.14 (*s*, 3H, *p*-Me (cymene)); 0.97 (*s*,6H, 2CH_3). ^{13}C NMR (400 MHz, DMSO-d_6). δ 166.74 (CH=N), 155.90 (C_2-Py), 154.57 (Py); 149.70 (Py); 139.88 (Py); 138.42 (Py); 137.58 (Ar); 130.24 (Ar); 129.76 (Ar); 128.71(Ar); 122.91(Ar);120.09 (Ar); 105.13 (Ar, *p*-cymene); 103.04 (Ar, *p*-cymene); 86.47(Ar, *p*-cymene); 85.80 (Ar, *p*-cymene); 85.30 (Ar, *p*-cymene); 85.19 (Ar, *p*-cymene); 30.46 (CH_3-, *p*-cymene); 21.74 (CH_3, *p*-cymene); 21.44 (CH_3, *p*-cymene); 19.52 (CH_3, *p*-cymene); 19.19 (CH_3), 18.21(CH_3). IR (KBr, cm^{-1}): 1610 (—CH=N), 830 (P-F). Anal. Calcd for [$C_{24}H_{28}ClN_2Ru$] PF_6 C, 46.05; H, 4.51; N, 4.48. Found: 45.10; H, 4.59; N, 4.64 .MS (ESI, *M*/*Z*): 481.0976 for [$C_{24}H_{28}ClN_2Ru$]$^+$

2.3. X-ray crystallography

Crystals of compounds **1a**, **1d** and **2c** suitable for X-ray diffraction studies were grown by slow diffusion of hexane layered over solutions of the compounds in dry acetone. Crystals were selected and glued onto the tip of glass fibres. The crystals were then mounted in a stream of cold nitrogen at 100(1) K and centred in the X-ray beam by using a video camera. The crystal evaluation and data collection were performed on a Bruker Smart *APE*X II diffractometer to crystal distance of 4.00 cm. The initial cell matrix was obtained from three series of scans at different starting angles. Each series consisted of 12 frames collected at intervals of 0.5° in a 6° range with the exposure time of about 10 s per frame. The reflections were successfully indexed by an automated indexing routine built into the *APEX* II programme suite [30]. The final cell constants were calculated from a set of 6460 strong reflections from the actual data collection. Data collection method involved ω scans of width 0.5°. Data reduction was carried out using the programme *SAINT*$^+$ [30]. The structure was solved by direct methods using *SHELXS* [31] and refined by *SHELXL* [30]. Non-H atoms were positioned geometrically and allowed to ride on their respective parent atoms. All H atoms were refined isotropically. The absorption correction was based on fitting a function to the empirical transmission surface as sampled by multiple equivalent measurements [30]. Crystal data and structure refinement information for compounds **1a**, **1d** and **2c** are summarized in Table 1.

2.4. General procedure for transfer hydrogenation of ketones

In a typical experiment the ketone (8.5 mmol), ruthenium(II) complex (0.00425 mmol) and NaOH (3.4 mmol) in 10 ml 2-propanol were introduced into a Schlenk tube fitted with a reflux condenser and heated to 82 °C in an inert atmosphere. The reaction was then monitored at various time intervals by the use of GC. This was achieved by taking an aliquot which was first passed through a pad of silica and then injected (0.1 μl) into the GC. The corresponding alcohol was the only product detected in all cases. The identity of the alcohol was confirmed by comparison with commercially available (Aldrich Chemical Co.) pure samples.

3. Results and discussions

3.1. Synthesis and characterization of cationic iminopyridyl Ru(II)-arene complexes

The mononuclear iminopyridyl complexes **1a–1d** and **2a–2d** were synthesized by stirring the ruthenium dimers [(η^6-arene)Ru(μ-Cl)Cl]$_2$ (where arene = C_6H_6 or *p*-cymene) with the corresponding *N*,*N*′-chelating ligand **a–d** respectively, in methanol or DCM at room temperature (Scheme 1).

The coordination of the ligand to form the complexes was confirmed by comparing the IR spectra, by looking at the

Table 1
Summary of the crystal data of **1a, 1d** and **2c.**

Compound	**1a**	**1d**	**2c**
Formula	$C_{26}H_{32}ClF_6N_2O_2PRu$	$C_{23}H_{26}ClF_6N_2OPRu$	$C_{22}H_{22}Cl_3F_6N_2PRu$
Formula weight	686.03	627.95	666.80
Crystal system	Orthorhombic	Triclinic	Monoclinic
Space group	P_2 1	$P\bar{1}$	P_21/n
a, Å	8.5619(11)	8.3236(9)	15.0341(4)
b, Å	17.074(2)	11.1178(12)	10.3961(3)
c, Å	19.680(3)	13.9567(15)	16.9722(3)
α,°	90	103.266(3)	89.086(2)
β, °	90	94.401(2)	75.128(2)
γ,°	90	98.746(2)	79.328(2)
V, Å ^{3}	2877.0(7)	1234.1	2471.74(12)
Z	4	2	4
D_{calcd}, mg/m^3	1.584	1.690	1.792
T, K	173(2)	173(2)	173(2)
μ, mm^{-1}	0.759x1	0.873	2.534
λ, Å	0.71073	0.71073	0.71073
F (000)	1392	632	1328
Cryst size, mm^3	0.08 × 0.09 × 0.17	0.16 × 0.17 × 0.18	0.180 × 0.140 × 0.097
θ_{min}, θ_{max},°	3.158–56.792	3.822–56.998	1.553–28.473
No. of reflns. collected	12327	49647	55748
No of indep. reflns.	6937	6221	6212[R(int)] = 0.0180]
Completeness to theta	100%	100%	100%
Absorbed correction	Semi-empirical from equivalents	Semi-empirical from equivalents	Semi-empirical from equivalents
Goodness-of-fit on F^2	1.027	1.051	1.065
Final R indices	0.0511, 0.1066	0.0266, 0.0614	0.0196, 0.0486
R indices (all data)	0.0679, 0.1156	0.0302, 0.0632	0.0234, 0.0510
Largest diff. peak & hole. Å^{-3}	1.27&−0.76	0.631&−0.45	0.607&−0.448

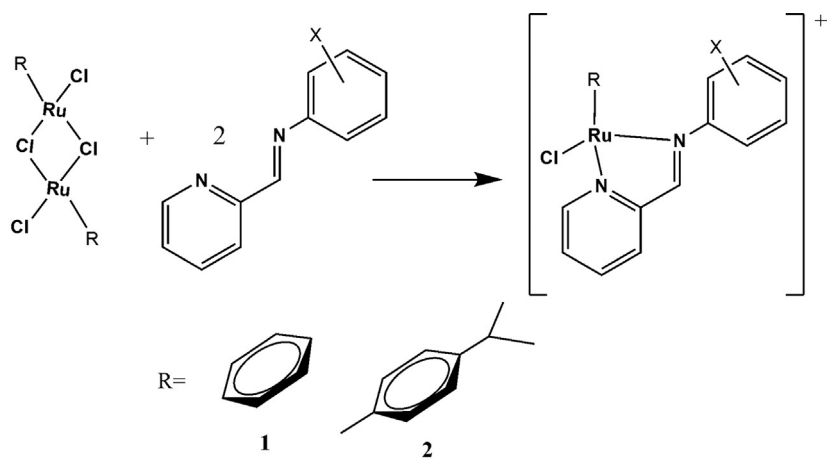

Scheme 1. Synthesis of [(η^6-R)RuCl(C_5H_4N-2—CH=N—C_6H_3X]PF_6 (*R* = C_6H_6 or *p*-cymene; *X* = 3, 5-dimethyl (**a**); 2,3-dimethyl (**b**); 2,5-dimethyl (**c**); 3,4-dimethyl (**d**)).

Table 2
Infrared wavenumbers for the imine functionalities for the compounds.

Imine functionality (cm^{-1})		
	Ligand	Complex
1a	1629.1	1609.3
1b	1631.8	1617.6
1c	1626.4	1616.7
1d	1629.0	1601.9
2a	1629.1	1607.8
2b	1631.8	1617.8
2c	1626.4	1611.2
2d	1629.0	1610.1

(C=N)$_{imine}$ stretching frequencies of the ligand and the complex. The (C=N)$_{imine}$ stretching frequencies for the complexes shifted to lower frequencies when compared to the ligand, suggesting coordination of the free ligands to the ruthenium centre (Table 2). These shifts are likely due to the (C=N) $_{imine}$ experiencing electron-withdrawing effects from the coordinated metal, which in turn weakens the (C=N) $_{imine}$ bond, leading to a shift to a lower frequency [32]. A sharp peak is also observed for all complexes in the region 840 cm^{-1} which can be attributed to the PF_6^- counter ion.

The ^{1}H NMR data for the [(η^6-C_6H_6)RuCl(C_5H_4N-2—CH=N-Ar]PF_6 (**1a–d**) complexes show a characteristic singlet assignable to the C_6H_6 protons at higher frequencies on bonding than the starting compound. The ^{1}H NMR data for the [(η^6-*p*-cymene)RuCl(C_5H_4N-2—CH=N-Ar]PF_6 (**2a–e**) complexes showed that resonances of the η^6-*p*-cymene protons were resolved to distinct peaks due to desymmetrization of the Schiff base at the ruthenium centre. This is in agreement with observation by other workers [18]. The imine proton (CH=N) of the complexes was observed as a singlet in the region δ 8.81 – 8.88 ppm, a shift downfield when compared to the ligands' imine peak (Table 3). This shift can be attributed to the deshielding of the amine proton as nitrogen donates its lone pair to the metal. In the ^{13}C NMR spectra

Table 3
^{1}H NMR and ^{13}C NMR shifts for the imine functionalities for compounds **1a–d** and **2a–d**.

Complex	^{1}H NMR		^{13}C NMR	
	Ligand	Complex	Ligand	Complex
1a	8.54	8.87	159.4	168.1
1b	8.53	8.81	159.7	171.5
1c	8.45	8.84	159.7	170.9
1d	8.54	8.86	160.1	166.9
2a	8.54	8.88	159.4	167.3
2b	8.53	8.83	159.7	171.2
2c	8.45	8.87	159.7	170.4
2d	8.54	8.87	160.1	166.7

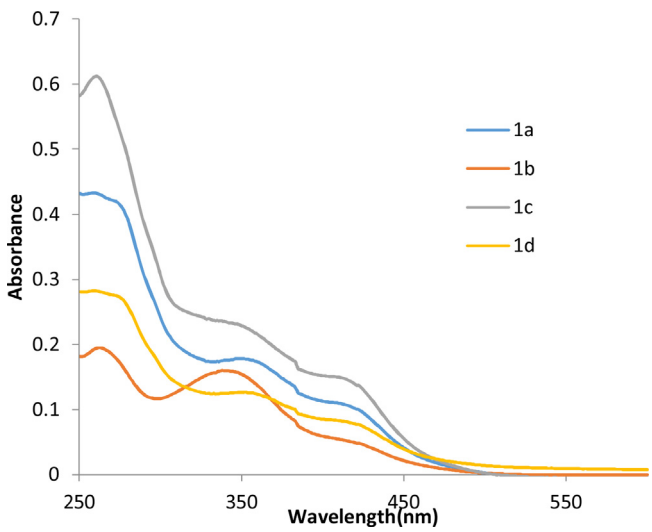

Fig. 1. UV–vis absorption spectra of mononuclear complexes **1a–d** in acetonitrile at 10^{-5} M concentration with 10 mm path length quartz cuvettes at 298 K.

of all the complexes, the —CH=N carbon shifts upfield for the complex as compared to the uncoordinated pyridine-imine ligand. This is probably due to a deshielding effect caused by increased charge transfer between the imine nitrogen and the ruthenium metal. The cationic complexes also display a septet in the ^{31}P NMR spectra for the cation PF_6^-, in the range of −131 to −151 ppm, which agrees with the literature values for other hexaflourophosphate salts [33].

ESI–MS typically revealed only one *M*/*Z* peak corresponding to the molecular ions [M$^+$] with the characteristic Ru isotopic pattern further confirming the formation of the complexes. All complexes show a base peak corresponding to the parent molecular ion without the PF_6^- counter ion.

UV–vis spectra of the complexes **1a–d** and **2a–d** were acquired in acetonitrile. Electronic spectra of the respective complexes are depicted in Figs. 1 and 2 Electronic spectra of all the mononuclear complexes displayed low intensity bands at 413–420 nm, medium intensity bands at 344–350 nm and high intensity bands at 263–267 nm. The low intensity band centred at 413–420 nm can be attributed to the metal-ligand charge transfer transition (MLCT) dπ–π*bands. This is due to the low spin d^6 configuration of the Ru(II) complexes which provides filled orbitals of proper symmetry on Ru(II) which can interact with the low lying π* orbitals on the pyridine-imine ligand. The medium intensity band at 344–350 nm and the high intensity bands at 263–265 nm are due to the ligand centred π–π* and π–π* transitions, in agreement with similar *N*,*N*′ bidentate ligands [34,35].

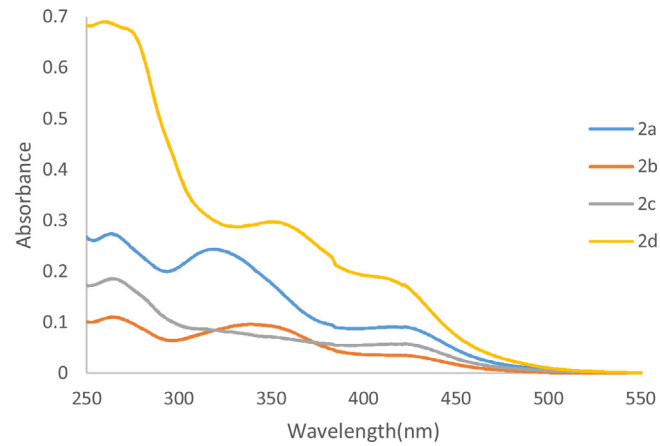

Fig. 2. UV–vis absorption spectra of mononuclear complexes **2a–d** in acetonitrile at 10^{-5} M concentration with 10 mm path length quartz cuvettes at 298 K.

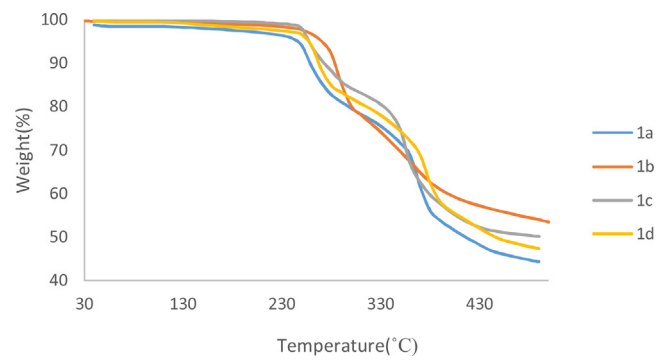

Fig. 3. TGA of **1a–d.**

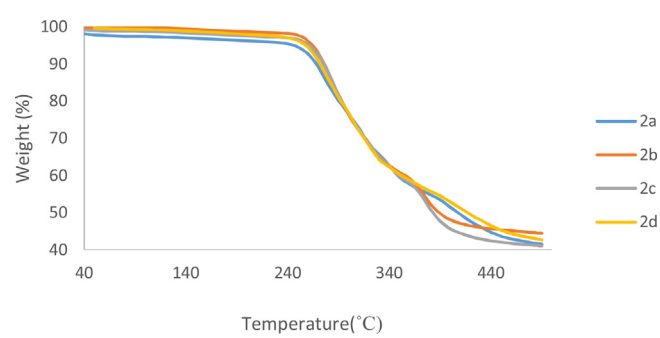

Fig. 4. TGA of **2a–e.**

3.2. Thermal gravimetric analysis

The compounds showed similar decomposition patterns, influenced by the arene ring. For the complexes with the benzene arene ring, two weight losses were observed between 220–310 °C corresponding to about 20% weight loss and between 290–400 °C corresponding to a 30% weight loss, which may be due to the loss of the arene and the bidentate ligand respectively (Fig. 3). The complexes with the *p*-cymene ring also had two weight losses (Fig. 4), between 220 and 370 °C corresponding to a 30% weight loss and 360–470 °C corresponding to a 20% weight loss, which may be attributed to the loss of the bidentate ligand and the *p*-cymene ring respectively. Similar two stage weight losses have also been reported for similar complexes [36].

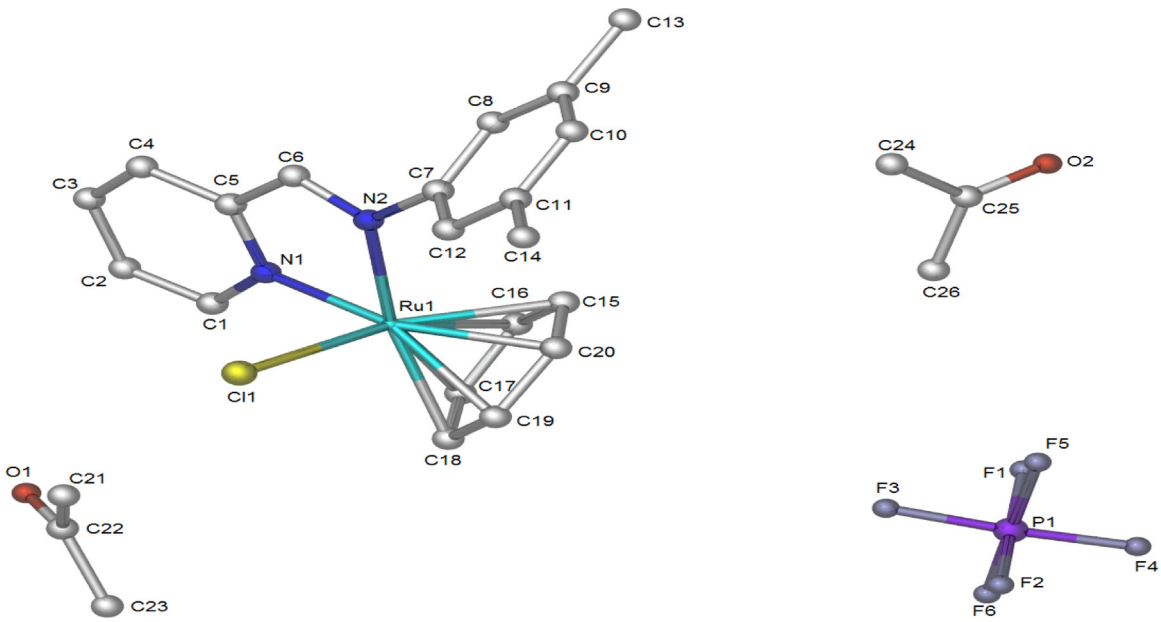

Fig. 5. The molecular structure of **1a** showing the atomic numbering scheme. Displacement ellipsoids are drawn at the 50% probability level and the C atoms are shown as small spheres.

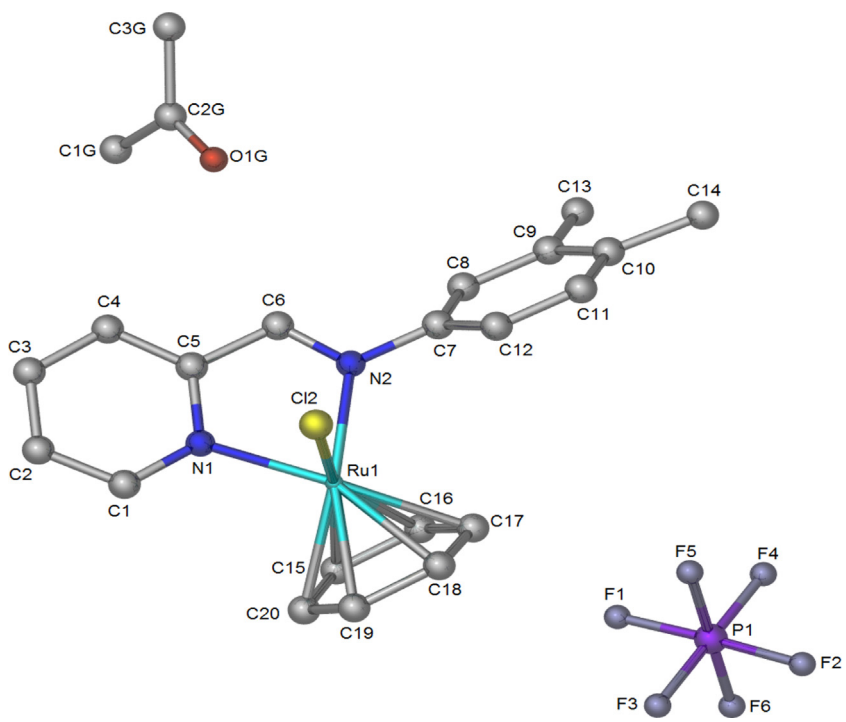

Fig. 6. The molecular structure of **1d** showing the atomic numbering scheme. Displacement ellipsoids are drawn at the 50% probability level and the C atoms are shown as small spheres.

3.3. Single crystal X-ray diffraction

The molecular diagrams of the cationic salts **1a**, **1d** and **2c** are shown in Figs. 5, **6** and **7**, while Table 4 gives a comparison of important bond distances and angles. The complex **1a** crystallized in an orthorhombic crystal system with a $P2_1$ space group, with one counter ion and two acetone molecule in each asymmetric unit, while **1d** crystallized as red blocks in the triclinic $P\bar{1}$ space group with one counter ion and an acetone molecule in each asymmetric unit. In addition the complex **2c** crystallize in the monoclinic P2/1n space group, with a counter ion in each asymmetric unit. The molecular structures of the complexes show the metal centre being coordinated by the *N*,*N*′-coordinating ligand and a terminal chloride which occupy the positions as the legs of the piano stool while the arene ring occupied the remaining coordination site as the seat of the piano stool. This arrangement is known as the pseudo-octahedral three legged piano stool structure. The Schiff—base ligand rotated slightly around N_2-C_7 to give a twisted conformation, presumably to reduce the steric interaction with the

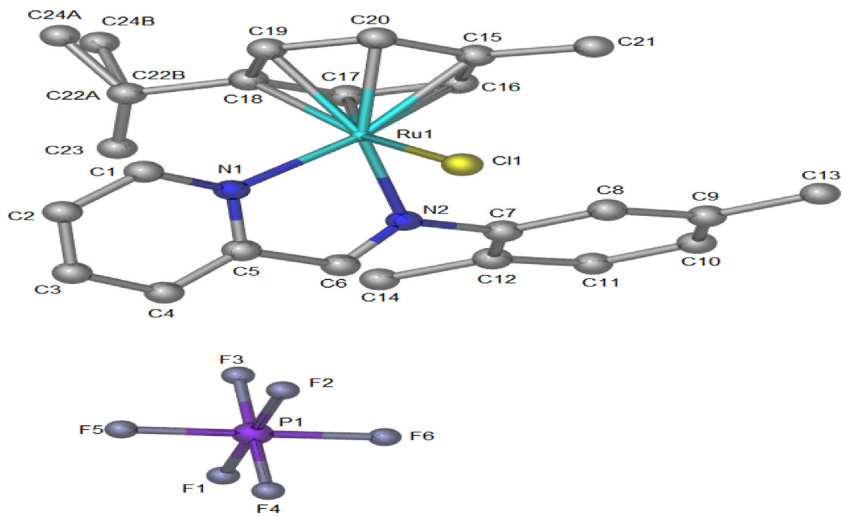

Fig. 7. The molecular structure of **2c** showing the atomic numbering scheme. Displacement ellipsoids are drawn at the 50% probability level and the C atoms are shown as small spheres.

Table 4
Selected bond lengths (Å) and angles (deg).

1a		**1d**		**2c**	
Bond Lengths		Bond Lengths		Bond Lengths	
Ru(1)—N(1)	2.0835(16)	Ru(1)—N(1)	2.0795(7)	Ru(1)—N(1)	2.0835(16)
Ru(1)—N(2)	2.0814(15)	Ru(1)—N(2)	2.0624(12)	Ru(1)—N(2)	2.0814(15)
Ru(1)—Cl(1)	2.3989(6)	Ru(1)—Cl(3)	2.380(7)	Ru(1)—Cl(1)	2.3989(6)
N(1)—C(5)	1.287(2)	N(2)—C(17)	1.285(3)	N(1)—C(15)	1.287(2)
N(1)—C(7)	1.437(2)	N(2)—C(16)	1.444(3)	N(1)—C(11)	1.437(2)
Bond angles		Bond angles		Bond angles	
N(1)—Ru(1)—N(2)	76.6(2)	N(2)—Ru(1)—N(1)	76.83(7)	N(1)—Ru(1)—N(2)	76.89(6)
N(1)—Ru(1)—Cl(1)	83.60(15)	N(1)—Ru(1)—Cl(3)	84.19(6)	N(1)—Ru(1)—Cl(1)	84.91(4)
N(2)—Ru(1)—Cl(1)	88.67(15)	N(2)—Ru(1)—Cl(3)	85.10(6)	N(2)—Ru(1)—Cl(1)	86.27(4)

cymene ligand. This is in agreement with observations of previous workers [18].

The bond distances Ru–N_{pyr} and Ru–N_{imine} of the complexes **1a** and **1d** and **2c** range from 2.0624 (12) Å to 2.095 (6) Å and are comparable to those reported for related compounds [18,37,38]. Similarly, the bond angles N_{pyr}-Ru-N_{imine} ranges from 76.6 (2) to 76.89 (6), while N_{py}-Ru-Cl ranges from 83.60°(15) to 84.91°(4) and N_{imine}-Ru-Cl ranges from 85.10°(6) to 88.67°(15) and are comparable to those of similar cationic complexes [39].

4. Catalytic properties

4.1. Optimization

The synthesized complexes were tested for the transfer hydrogenation of ketones. In order to optimize the reaction conditions, such as choice of base, temperature and catalyst loading, the transfer hydrogenation reaction of cyclohexanone to cyclohexanol was chosen as a model reaction. Temperature was found to have a strong influence on the performance of the catalyst, and when the reaction was carried out at ambient temperature low conversions were observed. However, raising the temperature to 82 °C gave good conversions and thus 82 °C was chosen for subsequent reactions. The conversion of cyclohexanone and the yield to cyclohexanol were found to be strongly dependent on the base employed. It was found that using strong inorganic bases like NaOH and KOH gave a remarkable increase in conversion and yield. NaOH gave the highest yields within the shortest reaction time. When weak inorganic bases, such as $NaHCO_3$ and tert-butoxide were employed, the conversions and yields were considerably reduced. Therefore NaOH was used for subsequent reactions. Next, the optimization of the base loading was carried out. A substrate to base loading ratio of between 2–8 was investigated. A substrate to base ratio of 4 was chosen, because less base resulted in lower conversions and yield, while a higher base concentration did not produce a considerable improvement in the conversion of cyclohexanone to cyclohexanol.

In addition, the catalyst loading was optimized and it was found that 0.05 mol% of the catalyst was most effective. Decreasing the amount to 0.025 mol % resulted in lower conversions and yield and increasing it to 0.1 mol% did not produce a considerable increase in conversion and yield. The ratio of the substrate/catalyst/base ratio was also optimized and was varied from 1/0.005/4 to 15/0.005/4. The ratio of 10/0.005/4 was chosen because at higher ratios the reaction took a long time to go to completion.

In addition, blank tests were done. Without addition of the base, no conversion was obtained. Also, using the base without the catalyst gave no appreciable conversions. Isopropanol was used as the hydrogen donor because it is readily available, inexpensive and easy to handle. Thus, the results of the optimization studies showed that the best yields were obtained using NaOH as the base in isopropanol solvent at 82 °C with 0.05 mol% of the catalyst. Thus, the optimum ratios for further catalytic applications were substrate/catalyst/base of 10/0.005/4.

Table 5
TH of cyclohexanone catalyzed by catalysts **1a–d** and **2a–d** in 2-propanol (S/C/B ratio is 10/0.005/4).

Catalyst	Substrate	Conversion(%)[a]	Time (h)	TON[b]	TOF[c]
1a	Cyclohexanone	98	2	1941	971
1b	Cyclohexanone	99	3	1900	633
1c	Cyclohexanone	99	3	1927	642
1d	Cyclohexanone	98	2	1965	982
2a	Cyclohexanone	97	2	1890	945
2b	Cyclohexanone	99	3	1927	642
2c	Cyclohexanone	98	3	1921	640
2d	Cyclohexanone	99	2	1920	960

[a] Conversion was determined by GC analysis using the internal standard method.
[b] Turnover number = mole of product/mol of catalyst.
[c] Turnover frequency = mole of product/mol of catalyst/hour (calculated when reaction deemed complete).

4.2. Catalytic results discussion

Under the optimized conditions, the transfer hydrogenation of cyclohexanone was carried out using the catalysts **1a–d** and **2a–d**. The results are presented in Table 5.

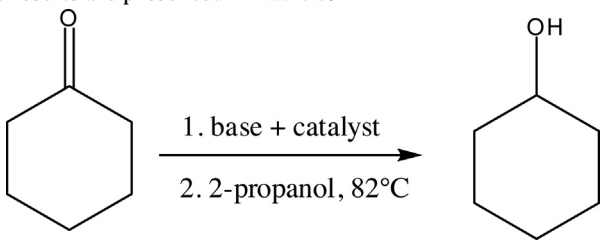

On comparing the effect of changing the arene substituents from benzene to *p*-cymene on the complexes, both showed high conversions within two to three hours. There was no significant effect on turnover numbers and turnover frequency. In addition, the effect of the changing the position of the electron donating methyl groups had an effect on the TOFs. The catalyst with the methyl substituents on the 3,5 and 3,4 positions had TOFs ranging from 945 to 982, while those with methyl substituents at positions 2,3 and 2,5 had TOFs ranging from 633 to 642. This implies that changing the methyl substitution from the 2 to the 3 position had some steric and electronic effect on the catalytic activity of the catalyst. The 2-methyl substituted ligands have stronger steric and electronic effect on the imine bond and thus have an influence on the loss of the chloride to form the catalytic intermediate. This may be due to the electron donating nature of the methyl group at the 2-position which affects the lewis acidity of the ruthenium centre, making it easier to form the hydride intermediate. The catalyst **1d** was chosen for the subsequent reactions because it showed the highest TON and TOF.

Under the optimized conditions, the transfer hydrogenation reactions of a range of ketones were investigated using catalyst **1d** in order to understand the scope and generality of this catalytic system. The ketones were chosen to explore the effects of electronic and steric variations on the substrate backbone. The results of this are presented in Table 6. Generally, cyclic aliphatic ketones gave higher conversion than the acyclic examples. This trend can be attributable to steric hindrance with respect to access to the C=O bond [7]. In addition, due to steric reasons, the effect of changing the location of the substituents from the 2 to 4 position of the cyclohexanone resulted in a significant increase in catalytic activity (Entries 1 and 2). A similar trend was observed by other researchers [7,40]. The ketones substituted in the 2-position showed the least reactivity of the cyclic compounds, likely due to a combination of steric interference of the substituents α to the reactive C=O bond and poor electron contribution from the methyl groups [7]. The straight chain ketones took a longer time to react compared to their cyclic

Table 6
Transfer hydrogenation of ketones catalyzed complex **1d**.

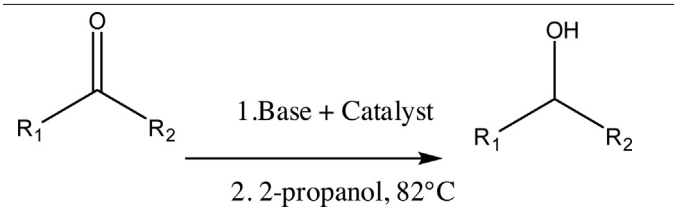

Entry	Substrate	Conversion (%)	Yield (%)	Time (h)	TON[b]	TOF[c]
1	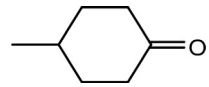	99	93	2	1852	926
2	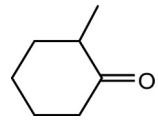	56	52	9[a]	1031	114
3	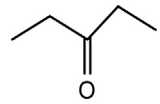	99	90	20	1790	90
4	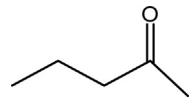	98	88	16	1768	110
5	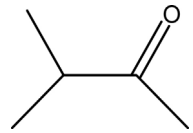	90	88	18	1810	100
6	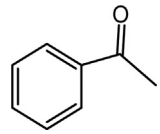	93	84	4	1660	415

[a] No further conversion noted with time.

counterparts. This may be attributed to the accessibility of the C=O bond in the rigid cyclic compounds as compared to the more sterically hindered reactive site in the straight chain ketone that led to a slower conversion to alcohols. It was also observed that ketones in which the C=O functional group was β to a CH_3 group (terminal; entry 4) were more reactive than internal C=O groups which are bonded to the ethyl group (entry 3). This showed that steric interactions were dominant factors for this catalysis and this trend has been reported by other researchers [41].

The TOFs obtained for the reaction of the diffrent ketones showed further the effect of the electronic and steric variations on the substrate backbone (Table 5). The cyclic aliphatic ketone substituted at the 4-position (Entry 1) showed a high TOF of 926 as compared to 2-methyl cyclohexanone which showed a TOF of 114. This may be attributed to steric hindrance on changing the substitution from 4 to 2 because substitution at the 2-position sterically hinders the reactive C=O group. On comparing the effect of changing the reactive C=O group from the terminal (Entry 4) and the internal (Entry 3) position, it was shown that the TOF for the ketone with the terminal C=O group was higher than the one with the internal C=O group. This may also be attributed to the steric hindrance.

No reaction was observed in the absence of the base. The base facilitates the formation of a ruthenium alkoxide by abstracting a proton from the alcohol and subsequently the alkoxide undergoes β-elimination to give a ruthenium hydride, which is an active species in this reaction. Assuming that these catalytic transformations follow the classical pathway in which the ketone

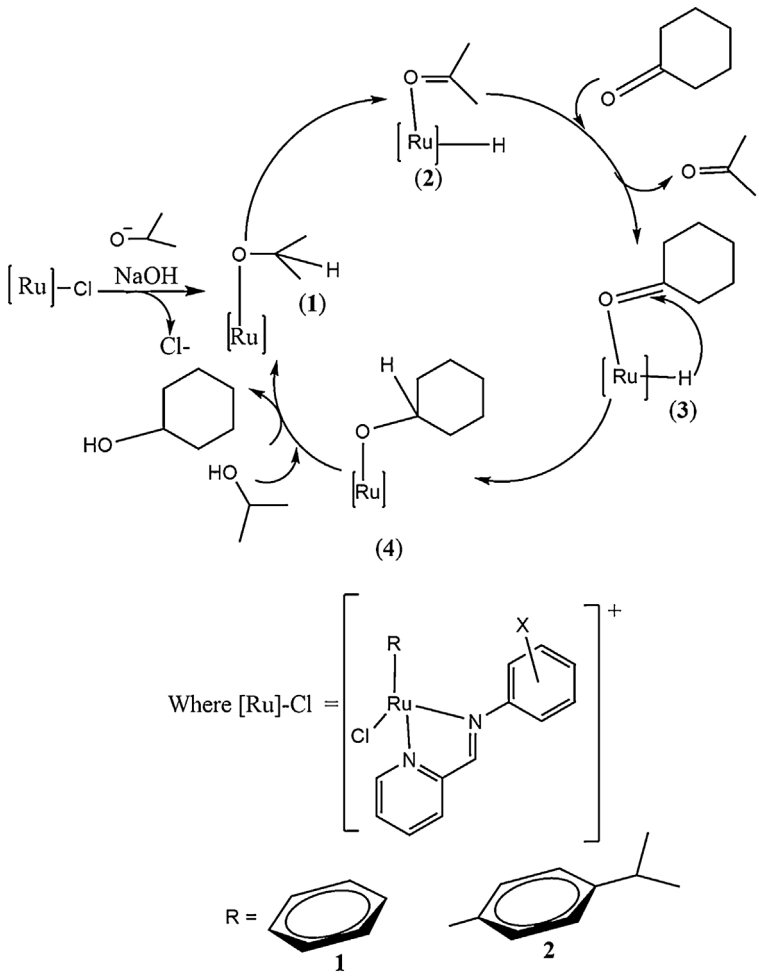

Scheme 2. Proposed mechanism for transition metal catalyzed transfer hydrogenation by complex **1** and **2**.

coordinates to ruthenium-hydride intermediates as proposed by several research groups [42–45], the observations seem to indicate that hydride transfer from the metal centre to the coordinated ketone is the rate limiting step (rather than ketone complexation) in the catalytic cycle [45].

The observation that no transfer hydrogenation occurs in the absence of the base suggests that the mechanism of the catalytic transformation most probably follows the classical pathway as is summarized in Scheme 2. In this mechanism the active species consists of an isopropoxide complex (**1**) which is readily formed in the presence of a base. This is followed by β-elimination in the presence of isopropanol which generates the hydride complex (**2**), to which cyclohexanone coordinates leading to the catalytic intermediate (**3**). Finally hydride transfer from ruthenium to the carbonyl group occurs to yield (**4**) which regenerates (**1**) by alkoxide exchange.

5. Conclusion

The compounds $[(\eta^6\text{-arene})RuCl(C_5H_4N\text{-}2\text{—}CH{=}N\text{-}R]PF_6$; where (arene = C_6H_6 (**1**), *p*-cymene (**2**), R = 3, 5-dimethyl phenyl (**a**), 2,3-dimethyl phenyl (**b**), 2,5-dimethylphenyl (**c**), 3,4-dimethylphenyl (**d**)) were synthesized from the $[(\eta^6\text{-arene})Ru(\mu\text{-}Cl)Cl]_2$ dimer with pyridine-2-carboxaldimines ligands. The structures of **1a**, **1d** and **2c** were confirmed, by single crystal X-ray diffraction, to have the pseudo-octahedral three legged piano stool geometry. The synthesized complexes were very effective catalysts in transfer hydrogenation of ketones using NaOH as the base. They showed high conversion and yield of the respective alcohols. Furthermore, catalyst also showed a wide scope, converting a variety of cyclic, aliphatic and aromatic ketones in 2-propanol as the hydrogen source and solvent.

Acknowledgements

We wish to extend our sincere thanks to the NRF, THRIP (Grant no. TP. 1208035643) and UKZN (URF) for financial support. JG thanks Prof. E. N. Njoka for his support.

Appendix A. Supplementary data

Supplementary data associated with this article can be found, in the online version, at http://dx.doi.org/10.1016/j.molcata.2016.02.012.

CCDC 1441202–1441204 contain the supplementary crystallographic data for this paper. These data can be obtained free of charge via http://www.ccdc.cam.ac.uk/conts/retrieving.html (or from the Cambridge Crystallographic Data Centre, 12, Union Road, Cambridge CB2 1EZ, UK. Fax: +44 1223 336033.

References

[1] L. Taghizadeh Ghoochany, C. Kerner, S. Farsadpour, F. Menges, Y. Sun, G. Niedner-Schatteburg, W.R. Thiel, Eur. J. Inorg. Chem. 2013 (2013) 4305.
[2] G. Zassinovich, G. Mestroni, S. Gladiali, Chem. Rev. 92 (1992) 1051.
[3] M. Aydemir, F. Durap, A. Baysal, N. Meric, A. Buldağ, B. Gümgüm, S. Özkar, L.T. Yıldırım, J. Mol. Catal. A: Chem. 326 (2010) 75.
[4] A. Nait Ajjou, J.-L. Pinet, J. Mol. Catal. A: Chem. 214 (2004) 203.
[5] H. Ji, Y. Huang, Y. Qian, T. Wang, M. Zhang, Chin. J. Chem. Eng. 14 (2006) 118.
[6] T.T. Upadhya, S.P. Katdare, D.P. Sabde, V. Ramaswamy, A. Sudalai, Chem. Commun. (1997) 1119.
[7] M.D. Bala, M.I. Ikhile, J. Mol. Catal. A: Chem. 385 (2014) 98.
[8] T. Marimuthu, H.B. Friedrich, ChemCatChem 4 (2012) 2090.
[9] X. Wu, J. Liu, D. Di Tommaso, J.A. Iggo, C.R.A. Catlow, J. Bacsa, J. Xiao, Chem. -A Eur. J. 14 (2008) 7699.
[10] K. Rafikova, N. Kystaubayeva, M. Aydemir, C. Kayan, Y.S. Ocak, H. Temel, A. Zazybin, N. Gürbüz, İ. Özdemir, J. Organomet. Chem. 758 (2014) 1.
[11] A. Aupoix, C. Bournaud, G. Vo-Thanh, Eur. J. Org. Chem. 2011 (2011) 2772.
[12] S. Ogo, K. Uehara, T. Abura, Y. Watanabe, S. Fukuzumi, Organometallics 23 (2004) 3047.
[13] C. Thoumazet, M. Melaimi, L. Ricard, F. Mathey, P. Le Floch, Organometallics 22 (2003) 1580.
[14] M.C. Carrión, F. Sepúlveda, F.A. Jalón, B.R. Manzano, A.M. Rodríguez, Organometallics 28 (2009) 3822.
[15] A. Bacchi, P. Pelagatti, C. Pelizzi, D. Rogolino, J. Organomet. Chem. 694 (2009) 3200.
[16] V.G. Vaidyanathan, B.U. Nair, J. Inorg. Biochem. 91 (2002) 405.
[17] L.J.K. Boerner, J.M. Zaleski, Curr. Opin. Chem. Biol. 9 (2005) 135.
[18] M.J. Chow, C. Licona, D. Yuan Qiang Wong, G. Pastorin, C. Gaiddon, W.H. Ang, J. Med. Chem. 57 (2014) 6043.
[19] A. Habtemariam, M. Melchart, R. Fernández, S. Parsons, I.D.H. Oswald, A. Parkin, F.P.A. Fabbiani, J.E. Davidson, A. Dawson, R.E. Aird, D.I. Jodrell, P.J. Sadler, J. Med. Chem. 49 (2006) 6858.
[20] P. Govender, A.K. Renfrew, C.M. Clavel, P.J. Dyson, B. Therrien, G.S. Smith, Dalton Trans. 40 (2011) 1158.
[21] B. Therrien, Coord. Chem. Rev. 253 (2009) 493.
[22] P. Kumar, R.K. Gupta, D.S. Pandey, Chem. Soc. Rev. 43 (2014) 707.
[23] A. Grabulosa, A. Mannu, E. Alberico, S. Denurra, S. Gladiali, G. Muller, J. Mol. Catal. A: Chem. 363-364 (2012) 49.
[24] C.G. Hamaker, D.P. Halbach, Polyhedron 28 (2009) 2228.
[25] P.G. Cozzi, Chem. Soc. Rev. 33 (2004) 410.
[26] C.-M. Che, J.-S. Huang, Coord. Chem. Rev. 242 (2003) 97.
[27] B.K. Dey, J. Dutta, M.G.B. Drew, S. Bhattacharya, J. Organomet. Chem. 750 (2014) 176.
[28] M.A. Bennett, A.K. Smith, J. Chem. Soc. Dalton Trans. (1974) 233.
[29] S. Dehghanpour, N. Bouslimani, R. Welter, F. Mojahed, Polyhedron 26 (2007) 154.
[30] Bruker-AXS Bruker-AXS, Madison, Wisconsin U.S.A., 2009.
[31] G. Sheldrick, Acta Cryst. A 64 (2008) 112.
[32] L.C. Matsinha, S.F. Mapolie, G.S. Smith, Polyhedron 53 (2013) 56.
[33] A.R. Burgoyne, B.C.E. Makhubela, M. Meyer, G.S. Smith, Eur. J. Inorg. Chem. 2015 (2015) 1433.
[34] A. Singh, N. Singh, D.S. Pandey, J. Organomet. Chem. 642 (2002) 48.
[35] G. Gupta, K.T. Prasad, B. Das, K.M. Rao, Polyhedron 29 (2010) 904.
[36] K.-G. Liu, X.-Q. Cai, X.-C. Li, D.-A. Qin, M.-L. Hu, Inorg. Chim. Acta 388 (2012) 78.
[37] R. Lalrempuia, M.R. Kollipara, P.J. Carroll, Polyhedron 22 (2003) 605.
[38] P. Govindaswamy, Y.A. Mozharivskyj, M.R. Kollipara, J. Organomet. Chem. 689 (2004) 3265.
[39] S.K. Mandal, A.R. Chakravarty, Polyhedron 11 (1992) 823.
[40] M.I. Ikhile, M.D. Bala, V.O. Nyamori, J.C. Ngila, App. Organomet. Chem. 27 (2013) 98.
[41] M.I. Ikhile, V.O. Nyamori, M.D. Bala, Tetrahedron Lett. 53 (2012) 4925.
[42] R. Noyori, S. Hashiguchi, Acc. Chem. Res. 30 (1997) 97.
[43] H. Doucet, T. Ohkuma, K. Murata, T. Yokozawa, M. Kozawa, E. Katayama, A.F. England, T. Ikariya, R. Noyori, Angew. Chem. Int. Ed. 37 (1998) 1703.
[44] E.P. Kelson, P.P. Phengsy, J. Chem. Soc. Dalton Trans. (2000) 4023.
[45] J.W. Faller, A.R. Lavoie, Organometallics 20 (2001) 5245.